17th International Symposium on Ballistics
Midrand, South Africa, March 1998

A HYDROCODE-DESIGNED WELL PERFORATOR WITH EXCEPTIONAL PERFORMANCE

David Davison (1) and Dan Pratt (2)

(1) Shock Transients, Inc., PO Box 5357, Hopkins, MN 55343 USA
(2) Owen Oil Tools, Inc., 8900 Forum Way, Ft. Worth, TX 76140 USA

The objective of the well perforator improvement effort was to increase the jet energy and penetration as much as possible while maintaining the same outer dimensions of the perforator body and limiting the explosive mass to 39 gm. The strategy was to replace the conical liner with a bell-shaped one of variable thickness, similar to ones that have shown significant gains in performance in prior studies. The outcome was an improved design that produced a jet with 10% more kinetic energy than before, with much of the increase at the back of the jet, where it was most effective in increasing the penetration depth. The penetration into the concrete target increased by 28% relative to the baseline.

The hydrodynamic computer program AUTODYN 2D™* and its thin-shell jetting option and the analytical penetration analysis program JEPETA™† were used to evaluate the baseline design and candidate alternative designs.

INTRODUCTION

Perforators, shaped charges for penetrating well casings and hydrocarbon-bearing rocks (Figure 1) must be low in cost yet effective to be marketable. The most critical component of the perforator is the liner, which is often fabricated by the low-cost process of pressing from a metal powder. For rocks of low porosity, the best perforations are ones that are as deep as possible.

Performance is characterized by testing against an American Petroleum Institute target (specifically, API RP-43 [API, 1991], Section 1) in which a thick layer of concrete simulates the hydrocarbon-bearing rock (Figure 2). The perforator's jet must penetrate the wall of a steel carrier, a fluid layer, and a steel wellbore casing before entering the concrete. An effective jet is one that creates a smooth, well-rounded hole through the casing as well as a deep, uniform hole in the concrete.

This paper reports the results of an effort to improve the penetration performance of a 2.11-inch diameter perforator with a steel body, loaded with 39 gm of HMX explosive. Figure 3 is a pair of conceptual diagrams of the baseline and the improved perforators. Features of the baseline and improved designs follow:

*AUTODYN 2D is a trade mark of Century Dynamics Inc.
†JEPETA is a trade mark of Shock Transients, Inc.

	Baseline	*Improved*
Liner Diameter	1.60 in (4.06 cm)	1.73 in (4.39 cm)
Liner Shape	Conical	Bell
Thickness Profile	Linear (Tapered)	Variable (Arbitrary)

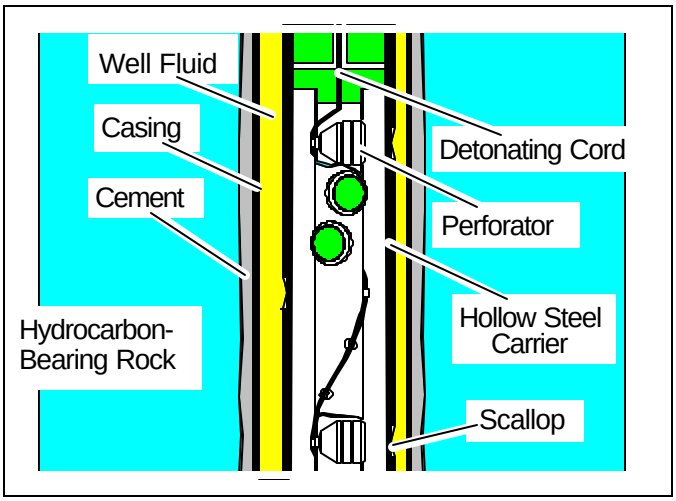

Figure 1. Section of a jet gun prior to firing. After a well is drilled, a steel casing is lowered into place and cement is pumped into the annulus between the casing and the rock. The jet gun is then lowered to the appropriate depth and fired to connect the hydrocarbon-bearing rock to the wellbore. The jet gun has a steel wall (hollow carrier) with thin, scalloped areas through which the perforators fire. Perforators are sequentially initiated with a detonating cord. Thick steel charge cases minimize charge-to-charge interference. In the diagram above, the gun is vertical, and perforators are oriented along vertical planes separated by an angle of 60º. After firing the jet gun, the hydrocarbon-bearing rock has many channels or perforations through which gas and/or oil flows into the wellbore.

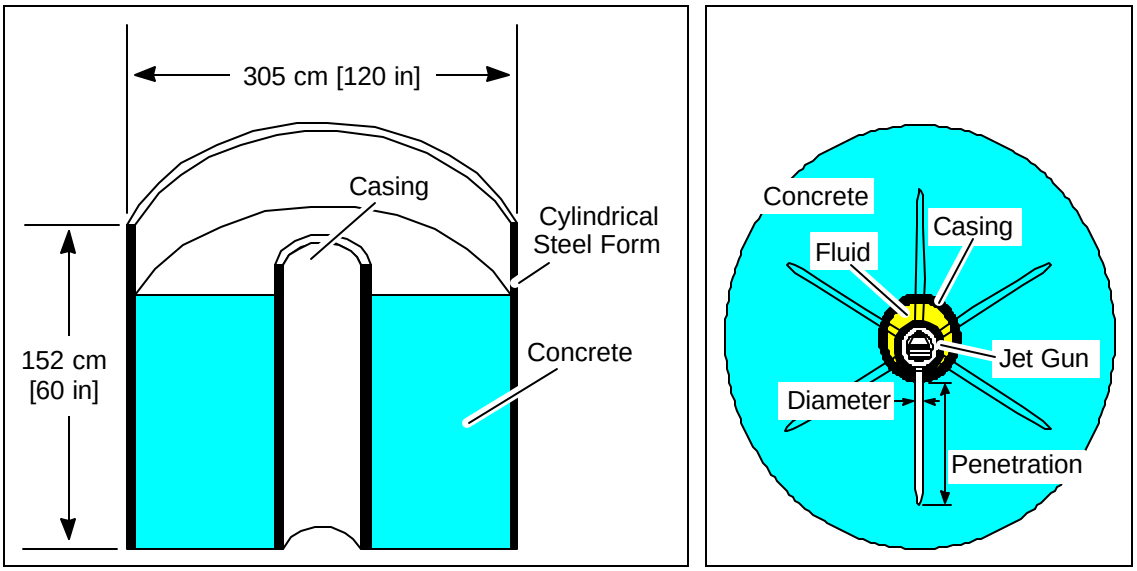

Figure 2. Perspective cutaway of the API RP 43, Section 1 target [API, 1991] and top view of the target showing the eccentric placement of the jet gun within the casing. For this work, the jet gun's outer diameter was 11.43 cm (4.50 inches) in diameter, and the casing's outer diameter was 17.78 cm (7.00 inches).

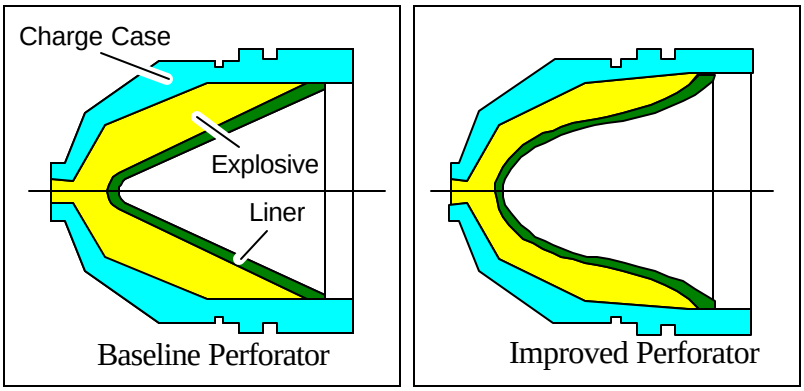

Figure 3. *Conceptual* diagrams of perforators; the actual liner shapes are proprietary. The baseline perforator has a conical liner of linear thickness variation, and the improved perforator has a bell-shaped liner of a slightly larger diameter, with a variable thickness. The improved liner's surface area is greater than that of the baseline, and points along the improved liner travel further than points along the baseline liner. All of these factors contribute to an improved jet that is more energetic than the baseline, and one that creates a deeper and wider perforation in concrete.

TEST RESULTS

The baseline and improved perforators were tested against the API target of Figure 2 and against the "quality control" (QC) target of Figure 4. Results were as follows:

	Target	*Baseline*	*Improved*
Entry Hole	API	0.46 in (1.17 cm)	0.37 in (0.94 cm)
Diameter	QC	0.54 in (1.37 cm)	0.35 in (0.89 cm)
Total Target	API	37.61 in (96 cm)	48.13 in (122 cm)
Penetration	QC	41.24 in (105 cm)	49.43 in (126 cm)
Diameter Hole at Bottom	QC	0.05 in (0.13 cm)	0.20 in (0.51 cm)

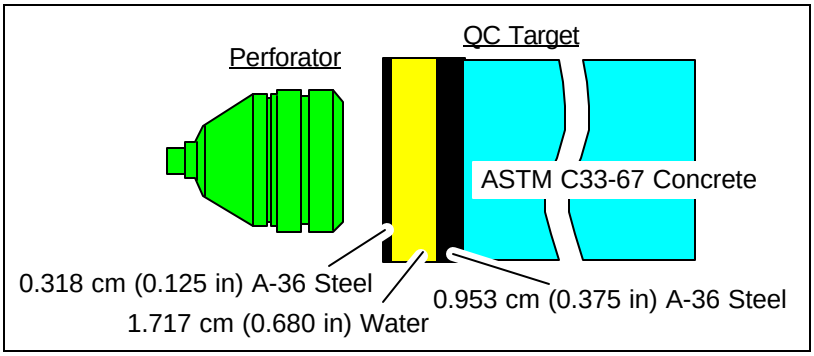

Figure 4. Perforator and cross-section of quality-control (QC) target; the QC target simulates the API RP 43 Section 1 target in preliminary testing. A single perforator is fired (vertically) through a target consisting of flat steel plates representing the gun wall and casing, enclosing water and backed up by stacked, four-inch diameter cylinders of cast concrete. The air gap between the perforator and the target was 1.575 cm (0.620 in) thick.

Perforations created by the baseline design tapered to a small diameter. Those created by the improved design were deeper and did not taper to a small diameter. The latter are more effective in bringing hydrocarbons (gas or oil) to the wellbore. The improved design has been named the Owen-STI NTX SDP™*. The "STI" in the name recognizes the contribution of Shock Transients, Inc., to the design; "NTX" stands for "New Technology, X Series;" and "SDP" stands for "super-deep penetrator."

THEORY

The improved perforator was designed to maximize its efficiency: the liner absorbed a greater amount of the explosive's energy than did the liner for the conventional, baseline perforator. Figure 5 is a plot of velocities as functions of time for several points along a liner. The plot illustrates the difference between the velocity histories for baseline and the improved perforators. Further details of the design process can be found in [Davison and Arvidsson, 1985] and [Davison and Nordell, 1992].

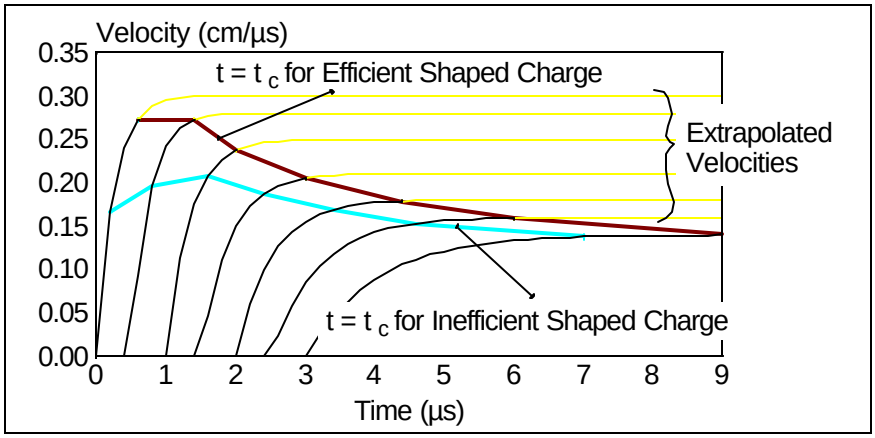

Figure 5. Velocity as a function of time for several points along a shaped charge liner. t_c, the collapse time, is the time at which the liner reaches the axis of symmetry, giving up its kinetic energy to the jet and slug. The kinetic energy of a jet element is proportional to that of the associated liner element at the moment of collapse, and the kinetic energy of a liner element is proportional to the square of its velocity. For an inefficient shaped charge the liner reaches the axis of symmetry while the velocity curve is steep. For an efficient shaped charge the liner reaches the axis of symmetry when the velocity curve has begun to level off. Shaped charges with bell-shaped liners are more efficient than those with conical or trumpet-shaped liners. The liner surface area is greater, and points along the liner are further from the axis of symmetry, allowing more time for the explosive to act on it.

The following is a summary of the shaped charge design approach: (1) Compute the perforator jetting with the definitive AUTODYN 2D program; (2) Compute the hole shape using the analytical penetration theory; (3) Derive liners that give jets of maximum energy and holes of maximum size; (4) Test the most promising designs; and (5) Iterate to converge on the "best" design(s).

Usage of AUTODYN 2D in shaped charge calculations is described in [Birnbaum and Cowler, 1989]. The liner is characterized as a jetting thin shell coupled to a fully two-dimensional representation of the explosive. The jet is modeled in accordance to the theory described in [Pugh et al., 1952].

*Owen-STI NTX SDP is a trade mark of Owen Oil Tools, Inc.

The JEPETA program takes the jet produced by the jetting thin shell model in AUTODYN 2D and computes its effect on a target. JEPETA includes the influence of target strength and jet breakup. It starts with the equations of [Eichelberger, 1956] and [Birkhoff et al., 1948] and continues with those of [Allen, 1977].

For JEPETA, the incremental penetration Δp is $\Delta p = \Delta L_j / n g$, where ΔL_j is the length of the jet increment including air spaces, ν is the ratio of ΔL_j to the length of the solid particles in the jet increment, and $g = \sqrt{r_t / r_j}$ for respective target and jet densities r_t and r_j. The incremental hole volume ΔV is proportional to the incremental jet kinetic energy; the ratio of energy to volume, E_S, is the target's specific energy. The jet's incremental kinetic energy depends on its incremental length, diameter, and velocity. The hole radius is $r_h = \sqrt{\Delta V / p \Delta p}$.

Some *focusing* (diameter reduction) of a powdered metal jet occurs when it passes through concrete and rocks such as sandstone and limestone [Aseltine, 1985]. In addition to focusing, rocks (and, to a lesser degree, concrete) also *disturb* jets, because of asymmetries and constrictions, reducing their effectiveness. When rocks contain hydrocarbons in their pores, the disturbance decreases, suggesting that *crushing* of the rock is a factor in the disturbance. Finally, jets are *disrupted* by reflections of shocks off target boundaries such as those of the QC configuration shown in Figure 4.

Of the four effects (focusing, disturbance, crushing, and disruption) observed and described by Aseltine, the first, focusing, causes the jet to be more effective than otherwise by concentrating the particles on the axis of symmetry. It remains dense and continuous, and it can be modeled as such in JEPETA.

The other three effects result from asymmetries or non-uniformities and are not modeled by the JEPETA computer program, which considers targets to be uniform and infinite in diameter. Consequently, JEPETA over-predicts penetration when these effects occur.

AUTODYN 2D ANALYSIS

The liners for the baseline and improved perforators were pressed from powdered metal, primarily tungsten and copper. The average density for the baseline liner was determined from the weight in air and in water to be 11.04 gm/cm³. Liners were sectioned axially into thirds, and densities for each third were measured. As indicated in Figure 6, a curve was fit through the data. The curve was used for making adjustments to thicknesses in the AUTODYN 2D analysis of the baseline so that the liner mass distribution would be correct. The adjustment was made in reverse to obtain the correct thicknesses for fabrication of the improved design.

Figure 7 is a set of velocity curves for the baseline and a set for the improved design. The following table lists features of the two jets:

Jet Feature	*Baseline*	*Improved*
Tip/Tail Velocity (cm/ms)	0.703/0.101	0.695/0.118
Mass (gm)	10.8	11.9
Kinetic Energy (kJ)	62.4	68.8

Both the mass and the kinetic energy of the jet from the improved design were 10% greater than that of the baseline. The increase was greatest at the aft end of the jet, which had the greatest effect deep within the target.

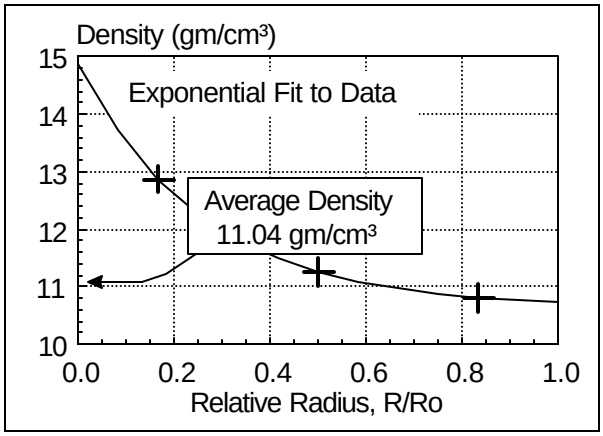

Figure 6. Liner density as a function of radius. Measured densities are marked with "pluses" on the figure above. The line is an exponential fit through the measurements. At each point, the thickness in the AUTODYN 2D calculation was adjusted by the ratio of the actual density to that assumed in the analysis to obtain the thickness for liner fabrication. This process assured that the masses in the AUTODYN 2D calculation were properly distributed along the liner.

Figure 8 is a pair of plots showing the theoretical hole shapes and energy depositions for the baseline and improved designs. For the JEPETA analysis, a jet density of 14.0 gm/cm³ and a breakup time of 140 μs were assumed. The breakup time value is large for a shaped charge of this size, but it is appropriate for a *focused* jet of powdered metal penetrating concrete, as discussed above. The constriction in the hole created by the baseline design appears to have disturbed the jet, making it less effective.

The API RP 43 test configuration of Figure 2 was assumed for the analysis. The following values were used:

		Density	*Strength*		E_S	*Thickness*	
Layer	*Material*	*(gm/cm³)*	*(kbar)*	*(kpsi)*	*(J/cm³)*	*(cm)*	*(in)*
Gap	Air	0.0013	–	–	–	1.575	0.620
Scallop	4140 Steel	7.86	10.3	150	4000	0.318	0.125
Fluid	Water	1.00	–	–	20	1.727	0.680
Casing	L80 Steel	7.86	6.2	90	3100	1.151	0.453
Concrete	ASTM C33-67	2.20	0.37*	5.4*	800	200	79**

*Compressive **Actual thickness of the API annulus is 55 inches

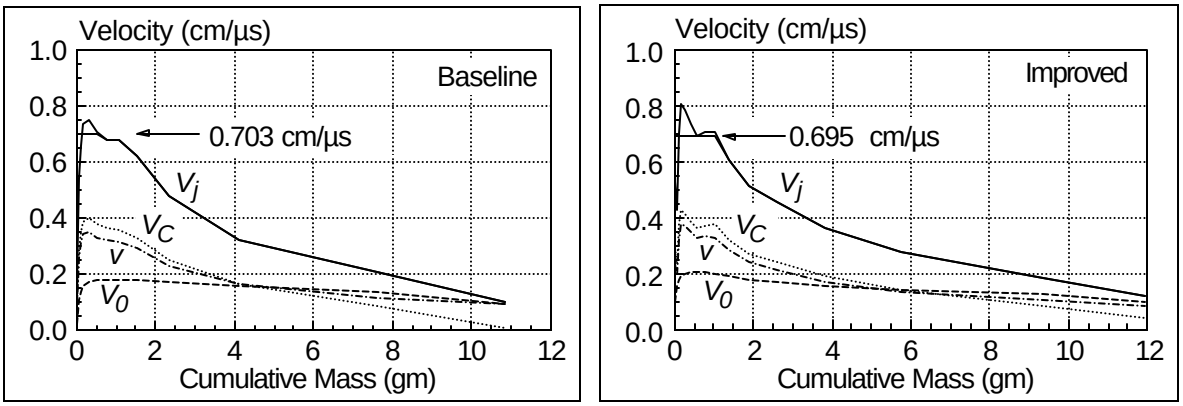

Figure 7. Velocities as functions of mass for the baseline and improved perforators. Plotted are the liner collapse velocity V_0, the relative velocity v, the stagnation point (collapse point) velocity V_C, and the jet velocity V_j. Note that $V_j = V_C + v$. The heavy line is the mass- or momentum-averaged jet velocity profile that results when fast particles at the back of the jet interact with slower ones in front; the resulting jet tip velocity is indicated.

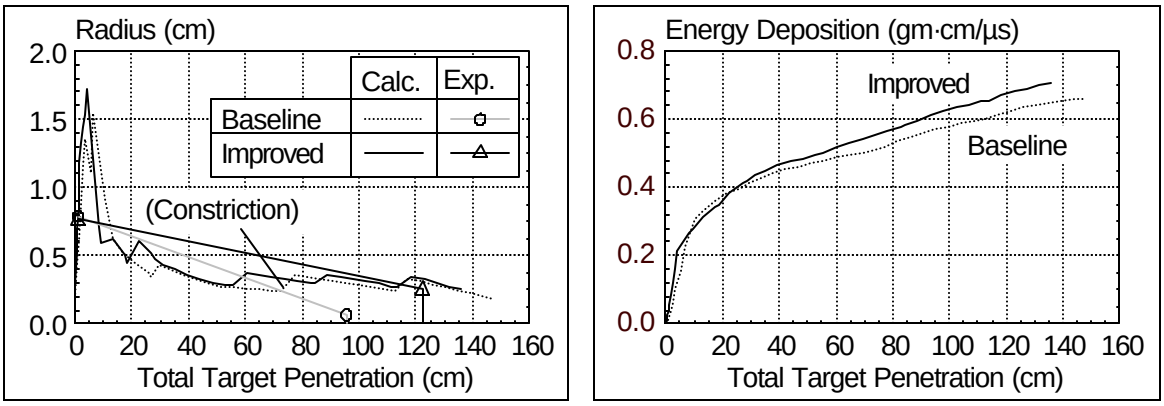

Figure 8. Theoretical hole profiles and energy depositions from JEPETA analysis and measurements on the holes in the experiments. Total target penetration starts at the face of the well casing (it includes the casing thickness). The energy deposition is the amount of jet kinetic energy required to reach a given penetration into the target. The radius of the hole tended to be greater for the improved design, and more energy was deposited deep in the target. The hole for the baseline design had a constriction at a penetration of approximately 70 cm that was eliminated by the improved design. Although the total target penetration computed by JEPETA for the baseline design (146 cm) was greater than the penetration computed for the improved design (135 cm), the experiments gave an opposite trend (96 cm for the baseline and 122 cm for the improved design).

The specific energy values for the metals in the table above are estimates based on published data for copper jets penetrating steel targets [DiPersio and Simon, 1968], adjusted by the inverse square root of the jet density, as suggested by hypervelocity impact data, for example [Maiden et al., 1960]. The 800 J/cm³ specific energy value for the concrete was estimated from the data reported here for the improved design. The 20 J/cm³ specific energy value for the water is hypothetical.

DISCUSSION

Using the hydrocode AUTODYN 2D, an improved design was derived that showed promise because it had a greater jet kinetic energy than the baseline and would use the additional energy deep within the target. The JEPETA calculations indicated that the improved design would widen the hole in cement, the nominal rock-simulating target medium, and would consequently decrease the disturbance to the jet as it created the perforation.

The experiments confirmed a wider hole and less disturbance, as evidenced by a 28% increase in the penetration. The productivity of an oil or gas well is proportional to the flow, which is primarily proportional to the depth of a perforation [Halleck and Dogulu, 1997]. Hence the 28% increase in penetration depth equates to a 28% increase in productivity.

In gas wells the velocity down a perforation and into the wellbore can be large in some cases, in particular, cases in which the wells have a large pressure drop between the rock and the wellbore and have holes through the casing that are reasonably large (that do not choke the flow). For these cases, the flow can be retarded by friction caused by roughness of the walls of the perforation. The retardation is reduced by increasing the diameter of the perforation. It follows that the improved perforator will be especially effective for gas wells of this type.

CONCLUSIONS

Calculations with AUTODYN 2D yielded an improved perforator design characterized by a potential to deposit a greater amount of energy deep within hydrocarbon-bearing rocks and their simulants (for example, concrete). Experiments comparing a baseline design to an improved design with 10% more jet kinetic energy confirmed that the depth and diameter of the perforation could be increased by this design strategy. The depth of the perforation increased by 28% and the diameter at hole bottom, by 300%.

REFERENCES

[Allen, 1977] F.J. Allen, *Discussion and Extension of Methods of Calculating Shaped Charge Jet Penetration*, BRL Memo Report 2773, July 1977. ADB020661.

[API, 1991] *Evaluation of Well Perforators*, Recommended Practice RP 43, American Petroleum Institute (API), January 1991.

[Aseltine, 1985] Aseltine, C.L., "Flash X-Ray Analysis of the Interaction of Perforators with Different Target Materials," *Proceedings of the 60th Annual Technical Conference and Exhibition*, SPE, September 1985. SPE Paper Number 14322.

[Birkhoff et al., 1948] G. Birkhoff, D.P. MacDougal, E.M. Pugh, and G. Taylor, "Explosives with Lined Cavities," *J. Appl. Phys.*, **19**, p. 563, June 1948.

[Birnbaum and Cowler, 1989] N. Birnbaum and M. Cowler, "A Combined Numerical/Analytical Approach for Shaped Charge Design," *Proceedings of the Eleventh International Symposium on Ballistics*, ADPA, Paper WM-20, v. 2, p. 179, May 1989.

[Davison and Arvidsson, 1985] D. Davison and B. Arvidsson, "Optimization of a 90 mm Shaped Charge Warhead" (with B.K. Arvidsson), *Second Symposium on the Interaction of Non-Nuclear Munitions with Structures*, USAF, p. 186, April 1985.

[Davison and Nordell, 1992] D. Davison and A. Nordell, "Optimization Process Giving an Exceptional Boost in Shaped Charge Jet Energy with No Weight Penalty," *Proceedings of the 13th International Symposium on Ballistics*, ADPA, Paper WM-27, v. 2, p. 521, June 1992.

[DiPersio and Simon, 1968] R. DiPersio and J. Simon, *The Effect of Target Hardness on the Penetration Capability of Shaped-Charge Jets*, BRL Report 1408, July 1968. AD 838991.

[Eichelberger, 1956] R.J. Eichelberger, "Experimental Test of the Theory of Penetration by Metallic Jets," *J. Appl. Phys.*, **27**, 1, p. 63, January 1956.

[Halleck and Dogulu, 1997] P.M. Halleck and Y.S. Dogulu, "The Basis and the Use of the API RP43 Flow Test for Shaped-Charge Oil Well Perforators," *Journal of Canadian Petroleum Technology*, **36**, 5, p. 53, May 1997.

[Maiden et al., 1960] C.J. Maiden, J. Charest, and H.P. Tardif, "An Investigation of Spalling and Crater Formation by Hypervelocity Projectiles," *Proceedings of the Fourth Symposium on Hypervelocity Impact*, v. 3, paper no. 38, April 1960.

[Pugh et al., 1952] E.M. Pugh, R.J. Eichelberger, and N. Rostoker, "Theory of Jet Formation by Charges with Lined Conical Cavities," *J. Appl. Phys.*, v. 23, no. 5, p. 532, May 1952.